struction of the immobile state. The fusion effect allows the peak intensity of the input sech^2 pulses to be reduced to non-propagating sub-threshold pulses so that a pair of these can generate a propagating soliton. This regime was observed in numerical simulations. The fusion occurs near the input facet of the system.

The set of equations (1) is known to have the following integrals of motion:

$$J_1 = \int \sum |B_j|^2 \, dz,$$

$$J_2 = \int \sum B_j(\partial B_j^*/\partial z) \, dz,$$

and

$$J_3 = \int \left[2D_1 \left| \frac{\partial B_1}{\partial z} \right|^2 + D_2 \left| \frac{\partial B_2}{\partial z} \right|^2 - \beta B_1^2 B_2^* - \beta B_1^2 + 2\Theta_1 \left| B_1 \right|^2 + \Theta_2 \left| B_2 \right|^2 \right] dz.$$

Negative value of J_3 guarantees self-trapping of immobile waves. For slow pulses J_3 possesses an additional positive contribution. Then, the condition for self-trapping requires modification of J_3. For the case of solitons with equal phase velocity ($D_1 = 2D_2$), we obtain: $\tilde{J}_3 = J_3 - D_1|J_2|^2/2J_1$. This modification is useful for predicting the evolution of a slow signal. A similar approach can be applied to spatial solitons propagating at different angles. The same modification could be made for solitons with cubic nonlinearities.[3]

This research was supported by INTAS (grant 97-0581) and RFBR (Russia).

Physics Department, Moscow State University, Vorobiovy Gory, Moscow, 119899, Russia; E-mail: aps@nls.phys.msu.su

1. Kivshar Yu. S. Phys. Rev. E. 1995. Vol. 51 (2). P. 1613.
2. Conti C., et al. Opt. Lett. 1997. Vol. 22 (7). P. 445.
3. Polyakov S.V., Sukhorukov A.P. Bull. Russ. Acad. Sci. Phys. 1998. Vol. 62 (12). P. 1849.
4. Conti C., et. al. Opt. Lett. 1998. Vol. 23 (19). P. 1514.

QWD15

Soliton pulse compression in optical parametric amplification

E. Ibragimov,* A. Struthers, D.J. Kaup,
Michigan Technological University, 1400 Townsend Dr., Houghton, Michigan 49931 USA; E-mail: struther@mtu.edu

Inverse Scattering Transform (IST) techniques, originating 20 years ago,[1] are applied to Optical Parametric Amplification (OPA). These techniques were extended to nonzero phase mismatch and applied to Sum Frequency Generation (SFG) and Second Harmonic Generation (SHG) in Ref. 2. There is currently a growing body of experimental results that we believe can be described by this theory.

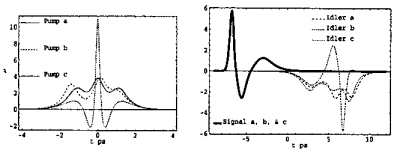

QWD15 Fig. 1. Numerical Verification of Stability of Signal (3 Solitons ± Radiation)

We consider a small, predelayed signal pulse (frequency ω_1 & velocity v_1) overtaking an intense pump (frequency $\omega_3 = \omega_1 \pm \omega_2$ & velocity v_3) in a χ^2 medium. An IST analysis of the Three Wave Interaction (TWI) equations shows intense pump pulses to be composed of numerous TWI-solitons. Each pump soliton can be thought of as a bound state (with zero binding energy) of energetically matched (by Manley-Rowe) signal and idler solitons. The small trigger initiates the decoupling by breaking the perfect energy balance and each pump soliton splits and emits one idler and one signal TWI-soliton.

The IST gives simple analytical expressions for the idler and signal output which reveal interesting features of the process. Specifically, the soliton decay process is extremely stable to perturbations of the pump and the signal output is independant of the initial pump shape. Figure 1 shows numerical verification of this analytical prediction with three distinct pumps producing identical signal output while the idler varies.

The analysis shows that the beneficial effects of Group Velocity Mismatch (GVM), described in Ref. 3 for SHG and explained in Ref. 2 using TWI-Solitons for both SHG and SFG, also exist for parametric processes. Our analysis shows that in parametric amplification the solitons emerge seperately with the most intense solitons appearing first. In fact, such a sequence of TWI-solitonswith the most intense soliton in the lead is clearly visible in the signal output in Fig. 1 where each of the three pumps contains three TWI-solitons. For intense pumps the duration of this dominant TWI-soliton can be more than an order of magnitude shorter than the pump duration. If the interaction is terminated after this soliton has emerged, the signal output has a smooth *sech* profile and can be up to 50 times shorter that the input pump. Using these results we explain experimentally observed pulse profiles and 20-fold compression.[4] Our investigation opens new possibilities for creating and shaping ultrashort pulses using parametric generation.

University of Maryland, Baltimore County, Baltimore, Maryland USA; E-mail: edibragi@mtu.edu

**Clarkson University Potsdam, New York, USA; E-mail: kaup@sun.mcs.clarkson.edu*

1. D.J. Kaup, A. Reiman, A. Bers, Rev. Mod. Phys., **51,** 275, (1979).
2. E. Ibragimov, A. Struthers, JOSA B, **14,** 1472 (1997).
3. A. Stabinis, G. Valiulis, E. Ibragimov, Opt. Comm., **86,** 301, (1991).
4. J.D.V. Khaydarov, J.H. Andrews, K. Singer, Optics Letters, **19,** 833 (1994).

QWD16

Soliton content with quadratic nonlinearities

D. Artigas, L. Torner, J.P. Torres,
D. Mihalache, D. Mazilu, *Laboratory of Photonics, Department of Signal Theory and Communications, Universitat Politecnica de Catalunya, Gran Capitan UPC-D3, Barcelona, ES 08034, Spain*

Quadratic solitons, that form through cascading in materials with second-order nonlinearities, are a topic of current intense investigation.[1] Solitons have been observed in second-harmonic generation (SHG) and in parametric amplification schemes, and many of their basic properties are well established. In particular, families of spatial and temporal solitons existing in waveguides and in bulk geometries are known, including those existing in settings with a small Poynting vector walk-off and/or temporal group-velocity mismatch. Under conditions where modulational instabilities can not grow, such families of solitons are stable under propagation and robust against several perturbations.

Notwithstanding, the evolution equations used to model soliton formation in quadratic nonlinear media do not belong to that special class of equations, referred to as completely integrable, that have soliton solutions in the rigorous mathematical sense. Therefore, the concepts and tools that are exclusive of integrable systems do not hold. In particular, contrary to integrable systems, the *soliton content* of an arbitrary signal, namely the fraction of the energy that corresponds to a soliton, is not known a priori.

On regard to quadratic solitons, in the actual excitation of solitons the shapes of the input signals are not necessarily close to those given by the soliton solutions of the governing equations. On the contrary, in the majority of cases, solitons are excited with inputs which fall very far from those solutions indeed. For example, because quadratic solitons are intrinsically multiple-wave entities, such is the situation encountered when light at only one of the involved frequencies, namely the funda-

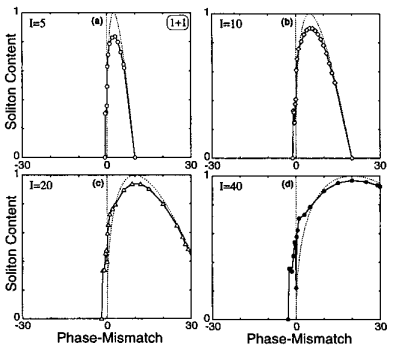

QWD16 Fig. 1. Fraction of the input light power carried by the excited solitons for different input powers, as a function of the phase-mismatch. The plot corresponds to spatial solitons that form in planar waveguides. Normalized input powers: (a) $I = 5$; (b) $I = 10$; (c) $I = 20$; (d) $I = 40$.

mental frequency or the second-harmonic when solitons are formed in SHG settings, is input to the crystal.

In this paper we report the results of comprehensive numerical investigations performed to evaluate the soliton content of several generic signal types and to elucidate its behavior as a function of the input light and material conditions. Figure 1 shows a representative example of the outcome. It shows the soliton content of sech-like input signals carrying different light powers as a function of the phase-mismatch between the multiple waves forming the solitons, in the case of (1 + 1) solitons that form in planar waveguides under conditions of SHG. In particular, the plot exposes that the soliton content is a narrow-band function of the phase-mismatch, with a power-dependent bandwidth and maximum reachable value. Results for (2 + 1) and (3 + 1) solitons are also presented.

1. For reviews, see G.I. Stegeman, D.J. Hagan, L. Torner, Opt. Quantum Electron. **28,** 1691 (1996); L. Torner, in Beam Shaping and Control with Nonlinear Optics, F. Kajzar and R. Reinisch eds., (Plenum, NY, 1998), pp. 229–258.

QWD17

Novel method for measuring Dicke narrowing by wavelength modulation spectroscopy

A.N. Dharamsi, A.M. Bullock, *Department of Electrical and Computer Engineering, Old Dominion University, USA; E-mail: dharamsi@ece.odu.edu*

Wavelength Modulation Spectroscopy signals exhibit features of frequency derivatives of the lineshape profile. Detection at the modulation frequency, f, yields signals that approximate the first derivative, and detection at the frequency Nf yields a signal that approximates the N^{th} derivative. Second harmonic (2f) detection[1,2] has been used frequently in the past, while we have recently demonstrated several advantages of higher harmonic detection.[3–5] These include an increased sensitivity to density fluctuations, and an increased resolution of overlapping lines.[6]

An examination of the dependence of the signal magnitude (which has been done for Voigt transitions) with pressure shows that, the signal magnitude grows initially with increasing pressure in the Doppler broadened region, and reaches a peak magnitude at a pressure $p_{\delta,N}$. It falls approximately as p^{-N}, in the collisional broadened regime. The familiar case of signal magnitude saturation in direct absorption is described in the theory developed, by using N = 0.[3–5]

We have extended the results discussed above by calculating the signal for non-Voigt profiles. Calculations were done assuming a Rautian-Sobelman profile, with various values of the narrowing parameter, α. A sample set of results for α = 0.00 (which is equivalent to the Voigt Profile), α = 0.01, and α = 0.03 cm^{-1} Atm^{-1} is shown in Fig. 1. For each value of α, calculations of the signal magnitude were performed for a range of pressures and detection harmonic orders of N = 1, 2, 3, 4 and 5.

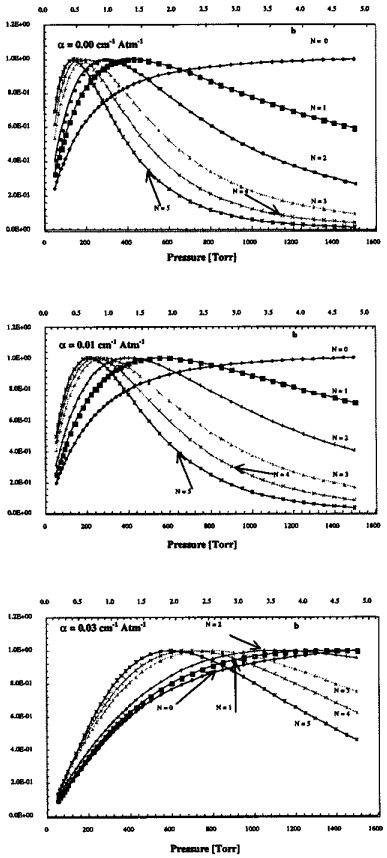

QWD17 Fig. 1. Calculated dependence of signal measured at various detection harmonic orders, N, on line narrowing parameter, α. Absorption transition used is the Oxygen A-Band RQ (13,14) line.

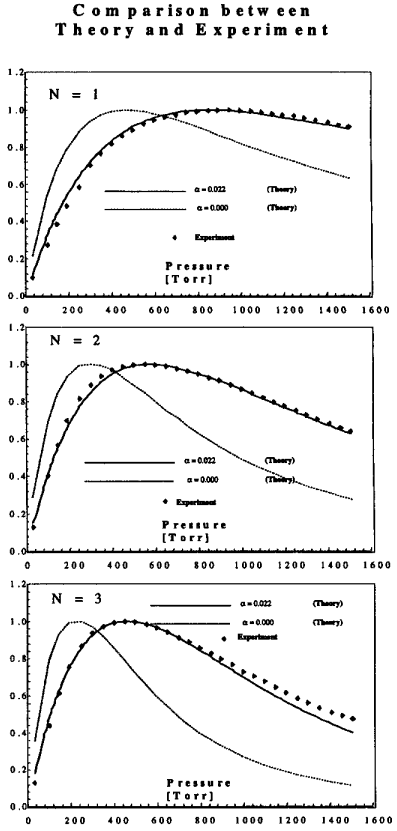

QWD17 Fig. 2. Experimental Results of measurements of signals obtained for harmonic detection orders up to the third (N = 3). Theoretical results for a Voigt profile (equivalent to α = 0) as well as α = 0.022 cm^{-1} Atm^{-1} is also shown. Measurements shown are for the Oxygen A-Band RQ (13,14) line.

An increasing value of α results in higher value of the pressure, $p_{\delta,N}$, at which the signal peaks, a result that can be understood *qualitatively* in a simple manner: For pressures less than $p_{\delta,N}$ one is in the Doppler regime. The signal magnitude begins to saturate (when N = 0) or decrease (for N = 1, 2, 3, . . .) as one approaches $p_{\delta,N}$, since, here, effects of collision broadening come into play. Dicke narrowing, as quantified by the narrowing parameter, α, counters collision-broadening effects, and $p_{\delta,N}$ should increase with increasing α, as the *quantitative* results of Fig. 1 verify.

Several lines of the Oxygen A-band were sampled in this manner and experiments were performed at various pressures. Harmonic detection orders of N = 1, 2, 3 were used at pressures ranging from 50 torr to approximately 1600 torr. Sample experimental and theoretical results for the Oxygen RQ[13,14] line of the A-Band line are shown in Fig. 2, which shows that the value of α = 0.022 cm^{-1} Atm^{-1} gives the best fit. The technique described here can be applied to a wide range of measurements that are of importance in environmental monitoring, industrial manufacturing and scientific applications. In all these applications, an accurate characterization of the lineshape function, including measurements of effects such as Dicke-narrowing, are of critical importance in obtaining accurate results.

1. J.A. Silver and A.C. Stanton, Appl. Opt., **27,** 1914, 1988.
2. G.V.H. Wilson, J. Appl. Phys. **34,** 3276, 1963.
3. A.N. Dharamsi and A.M. Bullock, App. Phys. Letts.; **69,** 22–24, 1996.
4. A.N. Dharamsi, J. Phys. D, Appl. Phys., **29,** 540, 1996.
5. A.N. Dharamsi and A.M. Bullock, App. Phys. B, Lasers and Optics, **63,** 283, 1996.
6. A.M. Bullock and A.N. Dharamsi, accepted for publication in J. Appl. Phys. (to appear Dec 15, 1998)

QWD18

The elementary theory of wavelet optical diffraction*

Tan Liying, Ma Jing, Ran Qiwen,* *National Key Laboratory of Tunable Laser Technology, Harbin Institute of Technology, 92 West Dazhi Street, 15001 Harbin, P.R. China*

Wavelet analysis is a new kind of analysis method and it shows better and better vitality in variety academic disciplines. In recent years,